arXiv:1211.0125v1 [cond-mat.supr-con] 1 Nov 2012

Spin-polarized Majorana Bound States around a Vortex in Topological Superconductors

Yuki Nagai, Hiroki Nakamura, and Masahiko Machida
CCSE, Japan Atomic Energy Agency, 5-1-5 Kashiwanoha, Kashiwa, Chiba, 277-8587, Japan
(Dated: November 2, 2012)

We analytically and numerically reveal that Majorana bound states inside the vortex core are distinctly spin-polarized in an odd-parity topological superconductivity classified as "pseudo-scalar" type of the gap function in massively Dirac-Bogoliubov-de Gennes (BdG) Hamiltonian constrained by strong spin-orbit coupling. This result is universal for "Dirac superconductivity" whose rotational degree of freedom is characterized by total angular momentum $J = S + L$ and in marked contrast to spin-degenerate core bound states given by the conventional BdG Hamiltonian. The spin-polarized vortex core can be easily detected by spin-sensitive probes such as neutron scattering and other measurements well above the first critical magnetic field H_{c1}.

PACS numbers: 74.20.Rp, 74.25.Op, 74.81.-g

The discovery of topological superconductor opened a new research avenue on superconducting states. The topologically-protected nature together with $U(1)$ broken symmetry produces Majorana fermions as gapless zero-energy quasi-particles at surface edges, while the superconducting gap opens in the bulk body. The emerged Majorana fermion is a counterintuitive particle whose annihilation and creation operators are identical. Such a unique particle has a promising role in topological quantum computing utilizing non-Abelian anyon statics. This fascinating novelty has highly stimulated many theorists and experimentalists to intensively study the topological superconductivity[1–11]. However, its research history is not so long as the topological insulator, and most of rich physics still remain elusive.

Very recently, Sasaki *et al.* found that 3-dimensional topological insulators, $\mathrm{Bi_2Se_3}$ and SnTe, turn into superconductors with carrier doping and moreover their superconducting gaps are not conventional since zero-bias conductance peaks (ZBCP's) can be detected by the point contact spectroscopy[12, 13]. The ZBCP is known to be observable in not only unconventional non-s-wave superconductors but also topological superconductors[12–17, 19]. A typical topological example is chiral p-wave superconductor such as $\mathrm{Sr_2RuO_4}$, in which gapless quasi-particles assigned as Majorana fermions induce ZBCP's[20–22]. Accordingly, ZBCP's observed in $\mathrm{Cu}_x\mathrm{Bi_2Se_3}$ ($T_c \sim 0.3$K) and $\mathrm{Sn}_{1-x}\mathrm{In}_x\mathrm{Te}$ ($T_c \sim 1.2$K) can be regarded to be originated from their non-trivial topology.

The Majorana fermion has been suggested to appear at not only surface edge but also vortex core in topological superconductors. Its emergence inside the vortex core has been numerically confirmed by using Bogoliubov-de Gennes (BdG) formalism for p-wave triplet superconductor[24**?**]. The vortex is basically a mobile object, indicating that Majorana fermion is also movable. The character is hopeful for the topological computing, since vortex manipulation techniques have been rapidly developed in the last decade. In this paper, we add a new insight on Majorana bound fermion inside the vortex core. We analytically and numerically reveal that the Majorana state is spin-polarized in topological superconductors originated from strong spin-orbit coupling. Such a case is not particular but rather universal, since the spin degeneracy supposed to be kept in the conventional BdG calculations is generally broken when spin and orbital angular momenta are coupled.

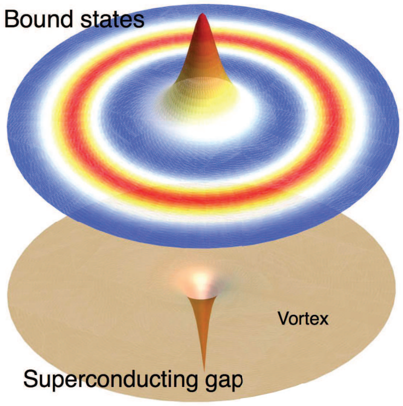

FIG. 1: (Color) Spin-polarized Majorana bound states. The red (blue) region denotes dominance of up-spin (down-spin) component.

A minimum model of topological superconductivity under strong spin-orbit coupling demands two orbital degrees of freedom in addition to two spin ones[4, 12, 25]. Then, the starting Hamiltonian corresponds to massive Dirac-type one including off-diagonal gap function, in which the Lorentz transformation invariance together with anti-commutation between two fermions gives a mathematical restriction on possible gap functions. As described in Ref. [26], the allowed gap function is characterized as a scalar, a pseudo-scalar, or polar-vectors when considering on-site Cooper pairing. The polar-vector case always produces a specific direction around which the rotational isotropy is broken in superconducting state. Consequently, the restriction allows six kinds of pairings, which are classified as two even-parity being not topological and four odd parity being topological. In $\mathrm{Cu}_x\mathrm{Bi}_2\mathrm{Se}_3$, Sasaki *et al.*, theoretically checked which type of these pairings successfully reproduces observed ZBCP's and suggested that the odd-parity spin-triplet pairing is most likely. Another superconductor, $\mathrm{Sn}_{1-x}\mathrm{In}_x\mathrm{Te}$ can be also examined by the same scheme. In this paper, we study vortex core bound-states in an odd-parity superconductivity whose gap function is characterized as "pseudo-scalar" keeping the rotational isotropy. In the case, the zero-energy Majorana bound states emerge at vortex cores as well as surface edges, and the core bound Majorana fermion is distinctly spin-polarized. In other topological cases, the spin-polarization becomes obscure since the rotational isotropy is broken around the vortex center and the polarized core states are mixed each other. We analytically and numerically demonstrate the result and discuss the theoretical mechanism as well as its experimental detection possibility.

An effective theory for the topological superconductor intrinsic to spin-orbit coupling is given by the massive Dirac type of BdG Hamiltonian together with Nambu representation for the two orbital degrees of freedom as

$$H = \int d\boldsymbol{r} \begin{pmatrix} \bar{\psi}(\boldsymbol{r}) & \bar{\psi}_{\rm c}(\boldsymbol{r}) \end{pmatrix} \begin{pmatrix} \hat{H}^{-}(\boldsymbol{r}) & \Delta^{-}(\boldsymbol{r}) \\ \Delta^{+}(\boldsymbol{r}) & \hat{H}^{+}(\boldsymbol{r}) \end{pmatrix} \begin{pmatrix} \psi(\boldsymbol{r}) \\ \psi_{\rm c}(\boldsymbol{r}) \end{pmatrix}, \tag{1}$$

where

$$\hat{H}^{\pm}(\boldsymbol{r}) = M(-i\boldsymbol{\nabla}) + \sum_{\nu=1}^{3} P_{\nu}(-i\boldsymbol{\nabla})\gamma^{\nu} \pm P_0(-i\boldsymbol{\nabla})\gamma^0. \tag{2}$$

Here, γ^i is 4×4 Dirac gamma matrix which satisfies the relations $\gamma^0 = \hat{\sigma}_z \otimes 1$, $\gamma^{i=1,2,3} = i\hat{\sigma}_y \otimes \hat{s}_i$ and $\gamma^5 = \hat{\sigma}_x \otimes 1$ with 2×2 Pauli matrices $\hat{\sigma}_i$ in the orbital space and $\hat{s}_i$ in the spin space, $\psi(\boldsymbol{r})$ is the Dirac spinor, $\bar{\psi}(\boldsymbol{r}) \equiv \psi^{\dagger}(\boldsymbol{r})\gamma^0$, $\bar{\psi}_c(\boldsymbol{r}) \equiv \psi_c^{\dagger}\gamma^0$, and $\psi_c \equiv \mathcal{C}\bar{\psi}^T$, where $\mathcal{C}(\equiv i\gamma^2\gamma^0)$ is the representative matrix of charge-conjugation. The gap functions are defined as $\Delta^- \equiv \gamma^0\hat{\Delta}i\gamma^2$ and $\Delta^+ \equiv \gamma^0(\Delta^-)^{\dagger}\gamma^0$, and M, P_ν, and ϵ are parameters depending on the materials. When considering only the on-site pairing interaction, the possible gap form is reduced into six types of functions as seen in Table I of Ref. [26]. These gap functions are classified into pseudo-scalar, scalar, and polar vector (four-vector) associated with the Lorentz transformation,

$$\Delta^- = \Delta_0,\ \Delta_0\gamma^5,\ \Delta_0\not{\alpha}\gamma^5, \tag{3}$$

where, Δ_0 is a scalar constant, the Feynman slash $\not{\alpha}$ is defined by $\sum_\mu \gamma^\mu\alpha_\mu$, and the gap function including $\not{\alpha}$ is characterized as unit four-vector α_μ. Since the vector type of the gap form represented by α_μ with finite α_i-components $(i = 1, 2, 3)$ points a specific direction, the rotational isotropy is broken around the direction resulting in the anisotropic quasi-particle spectrum in its superconducting states, even if the normal state is isotropic. This induced anisotropy yields the angle-dependent transport conductivity. For example, the anisotropic thermal conductivity is a clear evidence of the vector type of gap given by the four-vector α_μ [26].

From the Hamiltonian Eq. (1), the correspondent BdG equations are given as

$$\begin{pmatrix} \gamma^0\hat{H}^{-}(\boldsymbol{r}) & \gamma^0\Delta^{-}(\boldsymbol{r}) \\ \gamma^0\Delta^{+}(\boldsymbol{r}) & \gamma^0\hat{H}^{+}(\boldsymbol{r}) \end{pmatrix} \begin{pmatrix} u(\boldsymbol{r}) \\ u_{\rm c}(\boldsymbol{r}) \end{pmatrix} = E \begin{pmatrix} u(\boldsymbol{r}) \\ u_{\rm c}(\boldsymbol{r}) \end{pmatrix}. \tag{4}$$

Here, we note that v in the conventional eigen-state form, $(u, v)^T$ is given as $v \equiv i\gamma^2 u_c$.

Now, let us examine the vortex core bound states. Firstly, to analytically concentrate on the low-energy physics, we study the linearized Dirac Hamiltonian:

$$\hat{H}^{\pm}_{\rm eff}(\boldsymbol{r}) = M_0 - i\partial_x\gamma^1 - i\partial_y\gamma^2 - i\partial_z\gamma^3 \pm \mu\gamma^0, \tag{5}$$

with the renormalized axes $(x, y, z) \to (\bar{P}_1 x, \bar{P}_2 y, \bar{P}_3 z)$, where $\bar{P}_\nu$ is the coefficient of the linear term of $P_\nu(-i\boldsymbol{\nabla})$ in ν-direction, and μ denotes a chemical potential. For simplicity, we do not solve the gap-equation self-consistently and just give the spatial distribution of the order parameter around a single vortex $\Delta^-(\boldsymbol{r}) = \Delta^- f(r)e^{i\theta}$, where θ denotes the polar angle around c-axis (vortex line), $f(r)$ is the amplitude of the order-parameter ($f(r = 0) = 0$ and $f(r) > 0$).

At the zero energy, there is a relation expressed as $u_c(\boldsymbol{r}) = i\gamma^2 u^*(\boldsymbol{r})$, and the solution is expressed as $u(\boldsymbol{r}) = \zeta(r)u^{\rm N}(\boldsymbol{r})$, where $u^{\rm N}(r, \theta, z)$ is a solution in the normal states and $\zeta(r)$ is a scalar real function. In the case of the pseudo-scalar type of gap function $\hat{\Delta}_2 = \gamma^2\gamma^0$, there are two bound-state solutions at the zero-energy expressed as

$$u_{\uparrow}(\boldsymbol{r}) = \frac{e^{-K(r)}}{\sqrt{\lambda_+}} \begin{pmatrix} \sqrt{\mu + M_0}J_0(\bar{r}) \\ 0 \\ 0 \\ ie^{i\theta}\sqrt{\mu - M_0}J_1(\bar{r}) \end{pmatrix}, \tag{6}$$

$$u_{\downarrow}(\boldsymbol{r}) = \frac{e^{-K(r)}}{\sqrt{\lambda_-}} \begin{pmatrix} 0 \\ e^{i\theta}\sqrt{\mu + M_0}J_1(\bar{r}) \\ -i\sqrt{\mu - M_0}J_0(\bar{r}) \\ 0 \end{pmatrix}, \tag{7}$$

where $\bar{r} \equiv r\sqrt{\mu^2 - M_0^2}$, $K(r) \equiv \int_0^r |f(r')|dr'$ and $J_n(r)$ is the Bessel function of the first kind (See the supplemental material[29]). Here, $\lambda_\pm$ is determined by

$$\lambda_\pm = 4\pi \int_0^\infty dr r e^{-2K(r)} \left[(\mu \pm M_0)J_0(\bar{r})^2 + (\mu \mp M_0)J_1(\bar{r})^2\right]. \tag{8}$$

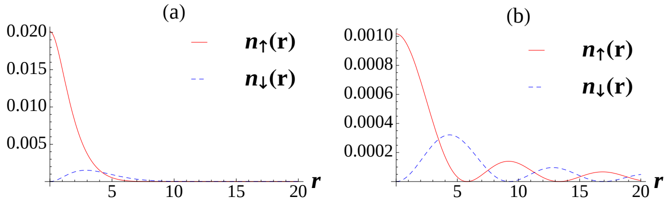

FIG. 2: (Color online) The radial dependence of the spin-resolved LDOS's with the gap-amplitudes (a) $\mu = 0.4$eV and $\Delta_0 = 0.3$eV, and (b) $\mu = 0.5$eV and $\Delta_0 = 0.01$eV.

We note that these two solutions are localized when $M_0^2 < \mu^2 + |\Delta_0|^2$[30]. Totally, we can obtain the solution at finite energy by a perturbation in terms of k_z. Assuming the solution $\psi(\boldsymbol{r})^T = c_\uparrow(u_\uparrow(\boldsymbol{r}), u_{c\uparrow}(\boldsymbol{r}))^T + c_\downarrow(u_\downarrow(\boldsymbol{r}), u_{c\downarrow}(\boldsymbol{r}))^T$, the dispersion relations are simply given by

$$E = \pm v k_z, \tag{9}$$

where the coefficients $(c_\uparrow, c_\downarrow) = (1, \pm i)/\sqrt{2}$ are not dependent on k_z, and

$$v \equiv \frac{2\pi\sqrt{\mu^2 - M_0^2}}{\sqrt{\lambda_+\lambda_-}} \int_0^\infty dr r e^{-2K(r)} \left(J_0(\bar{r})^2 - J_1(\bar{r})^2\right). \tag{10}$$

The spin-resolved local densities of states (LDOS's) $n_\uparrow(E = vk_z, r) \equiv |\psi_1(r)|^2 + |\psi_3(r)|^2$ and $n_\downarrow(E = vk_z, r) \equiv |\psi_2(r)|^2 + |\psi_4(r)|^2$ are expressed as

$$n_\uparrow(E = vk_z, r) \equiv \left(\frac{\mu + M_0}{2\lambda_\uparrow} + \frac{\mu - M_0}{2\lambda_\downarrow}\right) J_0(\bar{r})^2 e^{-2K(r)}, \tag{11}$$

$$n_\downarrow(E = vk_z, r) \equiv \left(\frac{\mu - M_0}{2\lambda_\uparrow} + \frac{\mu + M_0}{2\lambda_\downarrow}\right) J_1(\bar{r})^2 e^{-2K(r)}. \tag{12}$$

Here, $\psi_i(r)$ is the i-th component of the array solution form $\psi(\boldsymbol{r})$. We show r-dependence of $n_\uparrow$ and $n_\downarrow$ in two parameter sets with the assumption of the spatial form of the order-parameter $f(r) = r/\sqrt{r^2+1}$. As seen in Fig. 2(a), $n_\uparrow$ in $\mu = 0.4$ eV and $\Delta_0 = 0.3$ eV shows the peak structure at the vortex center ($r = 0$) in contrast to the zero density in $n_\downarrow$ because of $J_0(0) \neq 0$ and $J_1(0) = 0$. In $\mu = 0.5$ eV and $\Delta_0 = 0.01$ eV, which are the same as that in the previous papers [12, 26], $n_\uparrow$ and $n_\downarrow$ show qualitatively same similar distribution patterns as shown in Fig. 2(b). The integrated magnetization is also calculated by

$$M_z(r) = \int dk_z (n_\uparrow(k_z, r) - n_\uparrow(k_z, r)) \tag{13}$$

$$\sim m(n_\uparrow(E \sim 0, r) - n_\uparrow(E \sim 0, r)), \tag{14}$$

where m is a constant. Then, it is clearly found that the vortex core is spin-polarized as found from Fig. 2.

Next, we numerically calculate the LDOS's with the use of the material parameter sets for Cu$_x$Bi$_2$Se$_3$ to compare with the analytical results. We employ $L_x \times L_y$ triangle lattice grid. A single vortex center is located at $(i_x, i_y) = (L_x/2, L_y/2)$. To obtain the LDOS $n(\omega, i_x, i_y)$, we use the spectral polynomial expansion scheme[31–33] with 40 k_z-points and $L_x = L_y = 96$. We use renormalization factors $a = 30$ eV, $b = -\mu$, a smearing factor $\eta = 1 \times 10^{-3}$ eV, and a cut-off parameter $n_c = 8000$ (see, Ref. [31]). We take the gap-amplitude $\Delta_0 = 0.3$ eV and the chemical potential $\mu = 0.4$ eV, which are the same as the parameter sets of the analytical result in Fig. 2(a). Other parameters are the same as those in Ref. [26]. In the presence of a vortex, one can find the zero-energy bound states at the vortex core, in which there are the energy spectra of two bound states in the k_z-resolved LDOS's as shown in Fig. 3(a). One shows the linear dispersion relation around the zero-energy, while the other has a flat dispersion relation at the mid-gap energy ($E/\Delta_0 \sim 0.5$). We confirm that the k_z-dispersive spectrum consists of only up-spin quasiparticles while the mid-gap spectrum are opposite (See, Fig. 3(b)). As shown in Fig. 4, the r dependence of the spin-resolved LDOS at the zero-energy around a vortex shows that the vortex core is spin-polarized, which is consistent with our analytical calculation shown in Fig. 2(a).

Finally, we discuss the reason why the majorana fermion inside the vortex core is spin-polarized. First of all, we recall that the quasi-particle energy spectrum of the core bound state in topological superconductivity such as triplet p-wave one is given as $E_L \propto L$ where L is the orbital angular momentum in contrast to $E_L \propto (L + 1/2)$ in non-topological ones. Here, it should be noted that the above relation is valid when the full gap opens and the cylindrical symmetry is preserved around the vortex center. The above relation clearly indicates the presence of the zero-energy Majorana bound state at $L = 0$ in topological superconductivity. Then, we notice that the Majorana state is degenerated in terms of its spin momentum S in the conventional BdG scheme, resulting in no spin-polarization. On the other hand, when the spin-orbit coupling turns on, the preserved angular momentum L is replaced by the total one $J = L + S$. Then, a core bound state without the spin-orbit coupling is splitted by the spin degree of freedom into two states whose total angular momenta differ by $2S(= 1)$ and the mostly-bound Majorana state at the zero energy is a state of the splitted ones. Thus, one finds that the bound Majorana particle is distinctly spin-polarized. This consequence is universal and analogous to atomic orbitals when increasing the nuclear charge Z. The spin-polarized core is easily observable if vortex lattice is formed. For example, the neutron or muon scattering is sensitive to such a spin-density lattice like modulation, and NMR is

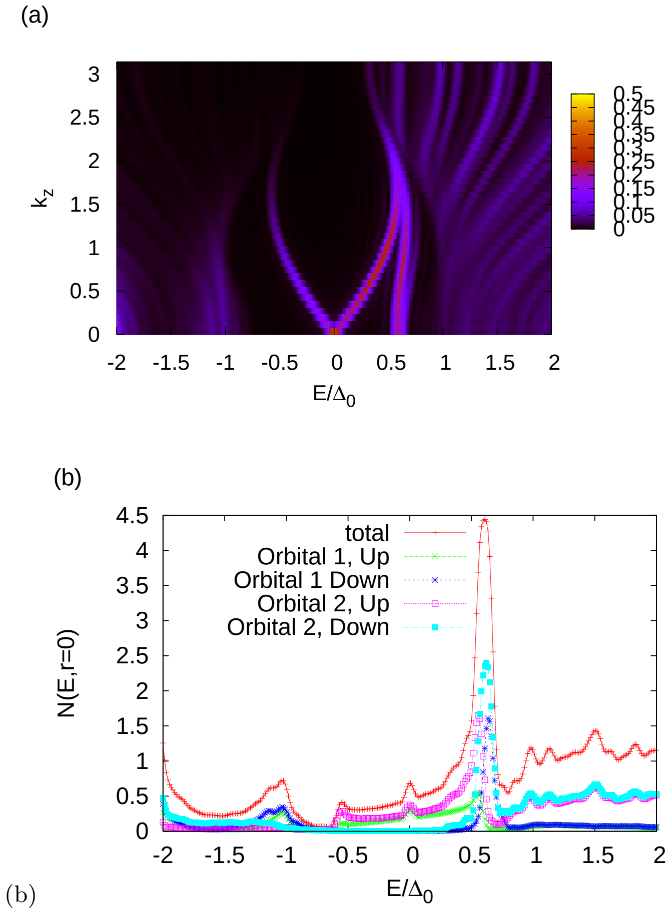

FIG. 3: The energy dependence of the LDOS's at the vortex center $(i_x, i_y) = (L_x/2, L_y/2)$ in the presence of a vortex in the superconductor whose the gap function Δ_2. (a) the k_z-resolved LDOS's. (b) the total and partial LDOS's.

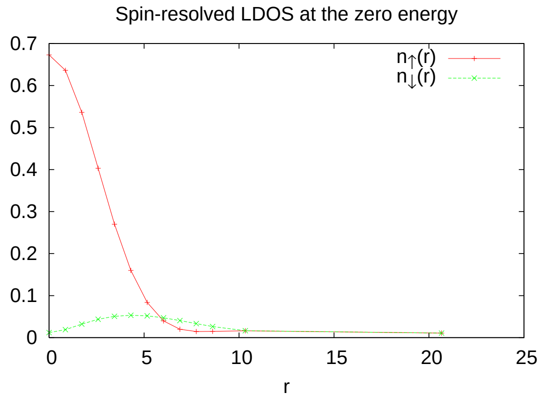

FIG. 4: The r dependence of the spin-resolved LDOS's at the zero-energy. r is determined by $r = \sqrt{3}(i_x - L_x/2)/(2\bar{A}_2)$. $i_y = L_y/2$.

also a good probe.

In conclusion, we obtained vortex core bound-states in a pseudo-scalar type topological superconductor using the model Hamiltonian of the topological superconductor $\mathrm{Cu}_x\mathrm{Bi}_2\mathrm{Se}_3$. We found that the zero-energy Majorana fermions are spin-polarized and the vortex core itself is magnetized. Such a drastic feature is easily observable in experiments.

We thank M. Okumura for helpful discussions and comments. The calculations have been performed using the supercomputing system PRIMERGY BX900 at the Japan Atomic Energy Agency.

[1] C. L. Kane and E. J. Mele, Phys. Rev. Lett. **95**, 146802 (2005).
[2] M. Z. Hasan and C. L. Kane, Rev. Mod. Phys. **82**, 3045 (2010), and references therein.
[3] B. A. Bernevig, T. L. Hughes, and S.-C. Zhang, Science **314**, 1757 (2006).
[4] L. Fu, C. L. Kane, and E. J. Mele, Phys. Rev. Lett. **98**, 106803 (2007).
[5] J. E. Moore, and L. Balents, Phys. Rev. B **75**, 121306(R) (2007).
[6] M. König, S. Wiedmann, C. Brüne, A. Roth, H. Buhmann, L. W. Molenkamp, X.-L. Qi, and S.-C. Zhang, Science **318**, 766 (2007).
[7] L. Fu and C. L. Kane, Phys. Rev. B **76**, 045302 (2007).
[8] A. Nishide, A. A. Taskin, Y. Takeichi, T. Okuda, A. Kakizaki, T. Hirahara, K. Nakatsuji, F. Komori, Y. Ando, and I. Matsuda, Phys. Rev. B **81**, 041309(R) (2010).
[9] T. Sato, K. Segawa, H. Guo, K. Sugawara, S. Souma, T. Takahashi, and Y. Ando, Phys. Rev. Lett. **105**, 136802 (2010).
[10] K. Kuroda, M. Ye, A. Kimura, S. V. Eremeev, E. E. Krasovskii, E. V. Chulkov, Y. Ueda, K. Miyamoto, T. Okuda, K. Shimada, H. Namatame, and M. Taniguchi, Phys. Rev. Lett. **105**, 146801 (2010).
[11] Y. L. Chen, Z. K. Liu, J. G. Analytis, J.-H. Chu, H. J. Zhang, B. H. Yan, S.-K. Mo, R. G. Moore, D. H. Lu, I. R. Fisher, S.-C. Zhang, Z. Hussain, and Z.-X. Shen, Phys. Rev. Lett. **105**, 266401 (2010).
[12] S. Sasaki, M. Kriener, K. Segawa, K. Yada, Y. Tanaka, M. Sato, and Y. Ando, Phys. Rev. Lett. **107**, 217001 (2011).
[13] S. Sasaki, Z. Ren, A. A. Taskin, K. Segawa, L. Fu, and Y. Ando, arXiv:1208.0059.
[14] Y. S. Hor, A. J. Williams, J. G. Checkelsky, P. Roushan, J. Seo, Q. Xu, H. W. Zandbergen, A. Yazdani, N. P. Ong, and R.J. Cava, Phys. Rev. Lett. **104**, 057001 (2010).
[15] L. A. Wray, S.-Y. Xu, Y. Xia, Y. S. Hor, D. Qian, A. V. Fedorov, H. Lin, A. Bansil, R. J. Cava, and M. Z. Hasan, Nature Phys. **6**, 855 (2010).
[16] M. Kriener, K. Segawa, Z. Ren, S. Sasaki, and Y. Ando, Phys. Rev. Lett. **106**, 127004 (2011).
[17] L. Fu and E. Berg, Phys. Rev. Lett. **105**, 097001 (2010).
[18] T. H. Hsieh, H. Lin, J. Liu, W. Duan, A. Bansil, and L. Fu, Nature Comm. **3**, 982 (2012).
[19] T. Kirzhner, E. Lahoud, K. B. Chaska, Z. Salman, A. Kanigel, arXiv:1111.5805.

[20] Y. Tanaka and S. Kashiwaya, Phys. Rev. Lett. **74**, 3451 (1995).

[21] Y. Nagai and N. Hayashi, Phys. Rev. B **79**, 224508 (2009).

[22] M. Sigrist, A. Furusaki, C. Honerkamp, M. Matsumoto, K.-K. Ng and Y. Okuno, J. Phys. Soc. Jpn. **89** (2000) Suppl. B 127.

[23] M. Takigawa, M. Ichioka, K. Machida, and M. Sigrist, Phys. Rev. B **65**, 014508 (2001).

[24] M. Matsumoto and R. Heeb, Phys. Rev. B **65**, 014504 (2001).

[25] L. Hao and T. K. Lee, Phys. Rev. B **83**, 134516 (2011).

[26] Y. Nagai, H. Nakamura, M. Machida, arXiv:1206.0563.

[27] D. Sticlet, C. Bena, and P. Simon, Phys. Rev. Lett. **108**, 096802 (2012).

[28] H. Zhang, C.-X. Liu, X.-L. Qi, X. Dai, Z. Fang, and S. C. Zhang, Nat. Phys. **5**, 438 (2009).

[29] See Supplemental Material at [URL will be inserted by publisher] for supplemental discussions.

[30] Y. Nishida, Phys. Rev. D **81**, (2010) 074004.

[31] Y. Nagai, Y. Ota and M. Machida, J. Phys. Soc. Jpn. **81**, (2012) 024710.

[32] Y. Nagai, N. Nakai and M. Machida, Phys. Rev. B **85**, (2012) 092505.

[33] L. Covaci, F. M. Peeters, and M. Berciu, Phys. Rev. Lett. **105**, (2010) 167006.

[34] A. Weisse, G. Wellein, A. Alvermann, and H. Fehske, Rev. Mod. Phys. **78**, (2006) 275.

Supplemental Material

S1. Solutions of the BdG equation around a vortex

Let us solve the following BdG equations:

$$\hat{H}\begin{pmatrix} u(\boldsymbol{r}) \\ u_c(\boldsymbol{r}) \end{pmatrix} = E\begin{pmatrix} u(\boldsymbol{r}) \\ u_c(\boldsymbol{r}) \end{pmatrix}, \tag{1}$$

where the Hamiltonian is

$$\hat{H} = \begin{pmatrix} \gamma^0\hat{H}^-(\boldsymbol{r}) & \gamma^0\Delta^-(\boldsymbol{r}) \\ \gamma^0\Delta^+(\boldsymbol{r}) & \gamma^0\hat{H}^+(\boldsymbol{r}) \end{pmatrix} = \begin{pmatrix} \hat{h}(\boldsymbol{r})-\mu & \Delta'(\boldsymbol{r}) \\ \Delta'^{\dagger} & \hat{h}(\boldsymbol{r})+\mu \end{pmatrix}, \tag{2}$$

with

$$\hat{h}(\boldsymbol{r}) = \gamma^0 M_0 - i\partial_x\gamma^0\gamma^1 - i\partial_y\gamma^0\gamma^2 - i\partial_z\gamma^0\gamma^3. \tag{3}$$

It should be noted that one can find the solution $(u^-, u_c^-) = (i\gamma^2 u_c^*, i\gamma^2 u^*)$ with the energy $-E$ when (u, u_c) is a solution with the energy E. The zero-energy solutions satisfy the following equations,

$$(\hat{h}-\mu)u + \Delta' i\gamma^2 u^* = 0, \tag{4}$$

$$\Delta'^{\dagger} i\gamma^2 u_c^* + (\hat{h}+\mu)u_c = 0. \tag{5}$$

We assume that these solutions are expressed as

$$u(\boldsymbol{r}) = \zeta(r)u^{\mathrm{N}}(r,\theta,z). \tag{6}$$

Here, $u^{\mathrm{N}}(r,\theta,z)$ is a solution in the normal states which satisfies

$$(\hat{h}-\mu)u^{\mathrm{N}}(\boldsymbol{r}) = 0. \tag{7}$$

At first, we solve the equation in the normal states. The equation is rewritten as

$$\hat{h}^2 u^{\mathrm{N}}(\boldsymbol{r}) = \mu^2 u^{\mathrm{N}}(\boldsymbol{r}), \tag{8}$$

$$(-\boldsymbol{\nabla}^2 + M_0^2)u^{\mathrm{N}}(\boldsymbol{r}) = \mu^2 u^{\mathrm{N}}(\boldsymbol{r}). \tag{9}$$

Thus, each component of the solution is expressed as

$$u^{\mathrm{N}i}(\boldsymbol{r}) = c_i e^{in_i\theta}J_{n_i}(\alpha r)e^{ik_z z}, \tag{10}$$

with $\alpha \equiv \sqrt{\mu^2 - M_0^2 - k_z^2}$. In order to obtain coefficients (c_1, c_2, c_3, c_4), we solve the following equations,

$$\begin{pmatrix} M_0 & 0 & k_z & L_- \\ 0 & M_0 & L_+ & -k_z \\ k_z & L_- & -M_0 & 0 \\ L_+ & -k_z & 0 & -M_0 \end{pmatrix}\begin{pmatrix} c_1 e^{in_1\theta}J_{n_1}(\alpha r) \\ c_2 e^{in_2\theta}J_{n_2}(\alpha r) \\ c_3 e^{in_3\theta}J_{n_3}(\alpha r) \\ c_4 e^{in_4\theta}J_{n_4}(\alpha r) \end{pmatrix} e^{ik_z z} = \mu\begin{pmatrix} c_1 e^{in_1\theta}J_{n_1}(\alpha r) \\ c_2 e^{in_2\theta}J_{n_2}(\alpha r) \\ c_3 e^{in_3\theta}J_{n_3}(\alpha r) \\ c_4 e^{in_4\theta}J_{n_4}(\alpha r) \end{pmatrix} e^{ik_z z}, \tag{11}$$

with

$$L_{\pm} \equiv \pm e^{\pm i\theta}(\mp i\frac{\partial}{\partial r} + \frac{1}{r}\frac{\partial}{\partial\theta}). \tag{12}$$

With the use of the relations $\partial_r J_n(r) = -J_{n+1}(r) + (n/r)J_n(r)$ and $\partial_r J_n(r) = J_{n-1}(r) - (n/r)J_n(r)$, we obtain

$$L_{\pm}e^{in\theta}J_n(\alpha r) = \pm e^{i(n\pm1)\theta}(\mp i\frac{\partial}{\partial r} + \frac{in}{r})J_n(\alpha r) \tag{13}$$

$$= \pm e^{i(n\pm1)\theta} i\alpha J_{n\pm1}(\alpha r). \tag{14}$$

Thus, the equations are rewritten as

$$\begin{pmatrix} (M_0-\mu)e^{in_1\theta}J_{n_1}(\alpha r) & 0 & k_z e^{in_3\theta}J_{n_3}(\alpha r) & -e^{i(n_4-1)\theta}i\alpha J_{n_4-1}(\alpha r) \\ 0 & (M_0-\mu)e^{in_2\theta}J_{n_2}(\alpha r) & e^{i(n_3+1)\theta}i\alpha J_{n_3+1}(\alpha r) & -k_z e^{in_4\theta}J_{n_4}(\alpha r) \\ k_z e^{in_1\theta}J_{n_1}(\alpha r) & -e^{i(n_2-1)\theta}i\alpha J_{n_2-1}(\alpha r) & (-M_0-\mu)e^{in_3\theta}J_{n_3}(\alpha r) & 0 \\ e^{i(n_1+1)\theta}i\alpha J_{n_1+1}(\alpha r) & -k_z e^{in_2\theta}J_{n_2}(\alpha r) & 0 & (-M_0-\mu)e^{in_4\theta}J_{n_4}(\alpha r) \end{pmatrix} \begin{pmatrix} c_1 \\ c_2 \\ c_3 \\ c_4 \end{pmatrix} = 0. \tag{15}$$

The orbital angular momenta n_i must satisfy

$$n_2 = n_1 + 1,\;\; n_3 = n_1,\;\; n_4 = n_1 + 1. \tag{16}$$

Then, in the case of $k_z = 0$, the coefficients are written as

$$c_3 = -\frac{ic_2\alpha}{M_0+\mu},\;\; c_4 = \frac{ic_1\alpha}{M_0+\mu}. \tag{17}$$

We assume that $\zeta(r)$ in Eq. (6) is a real scalar function. By substituting Eq. (6) into the differential equations Eq. (4), we obtain

$$\begin{pmatrix} ie^{-i\theta}\frac{\partial\zeta(r)}{\partial r}\frac{ic_1\alpha}{M_0+\mu}e^{i(n_1+1)\theta}J_{n_1+1}(\alpha r) \\ -ie^{i\theta}\frac{\partial\zeta(r)}{\partial r}\frac{ic_2\alpha}{M_0+\mu}e^{in_1\theta}J_{n_1}(\alpha r) \\ ie^{-i\theta}\frac{\partial\zeta(r)}{\partial r}c_2 e^{i(n_1+1)\theta}J_{n_1+1}(\alpha r) \\ ie^{i\theta}\frac{\partial\zeta(r)}{\partial r}c_1 e^{in_1\theta}J_{n_1}(\alpha r) \end{pmatrix} + \zeta(r)\Delta^{'}(r) \begin{pmatrix} \frac{-ic_1^*\alpha}{M_0+\mu}e^{-i(n_1+1)\theta}J_{n_1+1}(\alpha r) \\ \frac{-ic_2^*\alpha}{M_0+\mu}e^{-in_1\theta}J_{n_1}(\alpha r) \\ -c_2^* e^{-i(n_1+1)\theta}J_{n_1+1}(\alpha r) \\ c_1^* e^{-in_1\theta}J_{n_1}(\alpha r) \end{pmatrix} = 0 \tag{18}$$

Finally, we consider the gap function represented by s pseudo-scalar. In this case, $\Delta'(\boldsymbol{r})$ with a vortex is expressed as

$$\Delta'(\boldsymbol{r}) = f(r)e^{iM\theta}\gamma^0. \tag{19}$$

Here, M is a winding number and $f(r)$ is the amplitude of the order parameters ($f(r=0)=0$ and $f(r)>0$). By substituting $\Delta'(r)$ into the above differential equations, we obtain

$$\begin{pmatrix} i\frac{\partial\zeta(r)}{\partial r}\frac{ic_1\alpha}{M_0+\mu}e^{in_1\theta}J_{n_1+1}(\alpha r) \\ -i\frac{\partial\zeta(r)}{\partial r}\frac{ic_2\alpha}{M_0+\mu}e^{i(n_1+1)\theta}J_{n_1}(\alpha r) \\ i\frac{\partial\zeta(r)}{\partial r}c_2 e^{in_1\theta}J_{n_1+1}(\alpha r) \\ i\frac{\partial\zeta(r)}{\partial r}c_1 e^{i(n_1+1)\theta}J_{n_1}(\alpha r) \end{pmatrix} + \zeta(r)f(r) \begin{pmatrix} \frac{-ic_1^*\alpha}{M_0+\mu}e^{i(-n_1-1+M)\theta}J_{n_1+1}(\alpha r) \\ \frac{-ic_2^*\alpha}{M_0+\mu}e^{i(-n_1+M)\theta}J_{n_1}(\alpha r) \\ -c_2^* e^{i(-n_1-1+M)\theta}J_{n_1+1}(\alpha r) \\ c_1^* e^{i(-n_1+M)\theta}J_{n_1}(\alpha r) \end{pmatrix} = 0. \tag{20}$$

The angular momentum of the zero energy solutions is

$$n_1 = \frac{M-1}{2}. \tag{21}$$

Since $\zeta(r)$ is a scalar real function, we obtain two solutions with coefficients

$$(c_1, c_2) = (|c_1|\exp\left[\frac{\pi i}{4}\right], 0),\;\; (0, |c_2|\exp\left[-\frac{\pi i}{4}\right]). \tag{22}$$

Therefore, the zero-energy solutions with a winding number M are written as

$$u_\uparrow(\boldsymbol{r}) = c_\uparrow e^{-K(r)} \begin{pmatrix} \sqrt{\mu+M_0}\exp\left[i\frac{M-1}{2}\theta\right]J_{\frac{M-1}{2}}(\sqrt{\mu^2-M_0^2}r) \\ 0 \\ 0 \\ i\sqrt{\mu-M_0}\exp\left[i\frac{M+1}{2}\theta\right]J_{\frac{M+1}{2}}(\sqrt{\mu^2-M_0^2}r) \end{pmatrix}, \tag{23}$$

$$u_\downarrow(\boldsymbol{r}) = c_\downarrow e^{-K(r)} \begin{pmatrix} 0 \\ \sqrt{\mu+M_0}\exp\left[i\frac{M+1}{2}\theta\right]J_{\frac{M+1}{2}}(\sqrt{\mu^2-M_0^2}r) \\ -i\sqrt{\mu-M_0}\exp\left[i\frac{M-1}{2}\theta\right]J_{\frac{M-1}{2}}(\sqrt{\mu^2-M_0^2}r) \\ 0 \end{pmatrix}, \tag{24}$$

with $K(r) = \int_0^r |f(r')|dr'$.